



Influence of Al addition on structure and magnetic properties of nanocrystalline $\text{Fe}_{65}\text{Co}_{15}\text{Si}_5\text{Nb}_3\text{Cu}_1\text{B}_{11-x}\text{Al}_x$ alloys



Ying Han, Zhi Wang*, Yan-chao Xu, Zhong-yan Xie, Li-juan Li

School of Science, Tianjin University, Tianjin 300072, PR China

ARTICLE INFO

Article history:

Received 22 January 2016

Received in revised form 1 April 2016

Accepted 2 April 2016

Available online 8 April 2016

Keywords:

Nanocrystalline materials

FeCo-based alloy

Soft magnetic properties

Temperature dependence of permeability

ABSTRACT

The microstructure and soft magnetic properties of amorphous and nanocrystalline $\text{Fe}_{65}\text{Co}_{15}\text{Si}_5\text{Nb}_3\text{Cu}_1\text{B}_{11-x}\text{Al}_x$ ($x = 0, 1, 2, 3$) alloys were investigated. Microstructure has been analyzed from XRD patterns and magnetic properties were mainly studied by the evolution of initial permeability (μ_i) from room temperature to 700 °C. It was found that adding a certain amount of Al in $\text{Fe}_{65}\text{Co}_{15}\text{Si}_5\text{Nb}_3\text{Cu}_1\text{B}_{11}$ alloy significantly decreases onset primary crystallization temperature T_{x1} from 452 °C to 388 °C and increases the crystallized interval temperature ΔT_x from 188 °C to 290 °C. However, with the Al adding, the Curie temperature of amorphous phase T_c^m shows a decline tendency. After annealing at 550 °C, the alloy with $x = 1$ exhibited the maximum room-temperature μ_i , however, the most stable soft magnetic properties at elevated temperatures was found in the alloy with $x = 3$. Therefore, the (μ_i -T) curves of $\text{Fe}_{65}\text{Co}_{15}\text{Si}_5\text{Nb}_3\text{Cu}_1\text{B}_8\text{Al}_3$ samples annealed at 520–580 °C were also investigated in detail.

© 2016 Elsevier B.V. All rights reserved.

1. Introduction

Fe-based nanocrystalline alloys have several advantages over other classes of materials for soft magnetic applications. These include high initial permeability (μ_i), improved thermal stability compared with amorphous alloys and low core loss [1,2]. The lower Curie point of an amorphous matrix, T_c^m , however, limits its high temperature applications. It is well known that partial substitution of Fe by Co in Finemet alloys could enhance the Curie temperature of amorphous phase [3–5], but superfluous Co doping into Finemet would damage the magnetic softness because of larger magnetostriction. Therefore, a small amount of Co doping into Finemet is expected for improving both room- and high-temperature magnetic softness. In nanocrystalline alloys, the substitution of Co for Fe can also raise the saturation magnetization substantially, but this effect is diminished when the alloy also contains Si [4–8]. Furthermore, a high Si content will decrease the amorphous forming ability of the alloy which is made by the alloy composition deviation from the eutectic point. Therefore, a small amount of Si content is necessary for improving magnetic softness of nanocrystalline alloy with low Co content.

It is reported that addition of Al in Finemet alloys could exhibit a lower H_c and a higher permeability due to the reduction in K_1 and ultimately improve soft magnetic properties [9,10]. However, the change in magnetic properties with B and Al variation in the FeCoNbCuSiB system and their correlation with the structure has not been studied systematically so far. In addition, the Curie temperature of the crystalline phase

and the magnetization in annealed samples abruptly decreased, when there was more than 5 at.% of Al in the alloy [11]. Therefore, a certain amount of Al was selected for partly substituting B in $\text{Fe}_{65}\text{Co}_{15}\text{Si}_5\text{Nb}_3\text{Cu}_1\text{B}_{11}$ alloy and a series of $\text{Fe}_{65}\text{Co}_{15}\text{Si}_5\text{Nb}_3\text{Cu}_1\text{B}_{11-x}\text{Al}_x$ ($x = 0, 1, 2, 3$) alloys were fabricated. In present research, the influence of Al addition on the microstructure and magnetic properties at room- and high-temperatures of FeCo-based Finemet-type alloys was mainly investigated.

2. Experimental procedures

Amorphous ribbons of 0.8–1 mm wide and about 30 μm thick, were obtained by the single-roller melt spinning method with nominal composition $\text{Fe}_{65}\text{Co}_{15}\text{Si}_5\text{Nb}_3\text{Cu}_1\text{B}_{11-x}\text{Al}_x$ ($x = 0, 1, 2, 3$). The systematic errors were mainly obtained by material purity (99.99%) and measuring instrument precision (0.0001 g). The toroidal samples with an outer diameter of about 18 mm and inner diameter of about 16.3 mm were fabricated by winding the ribbons into toroidal cores. To obtain the characteristic nanocrystalline structures, samples were submitted to isothermal annealing at 520–580 °C for 0.5 h under vacuum atmosphere. The phase structure of 550 °C-annealed ribbons was examined by x-ray diffraction (XRD) using D/max-2500/PC with Cu-K α radiation ($\lambda = 1.54056 \text{ \AA}$). The initial permeability μ_i was in situ measured by HP4294A impedance analyzer at $H = 0.4 \text{ A/m}$, $f = 10 \text{ kHz}$ and a heating rate of 10 °C/min under Ar atmosphere protection over the temperature range of 30–700 °C. The systematic errors mainly produced by temperature deviation were estimated about 5%. The saturation magnetization B_s was measured by vibrating sample magnetometer (VSM). The crystallization temperature of amorphous ribbons (T_x) was determined by

* Corresponding author.

E-mail address: zhiwang@tju.edu.cn (Z. Wang).

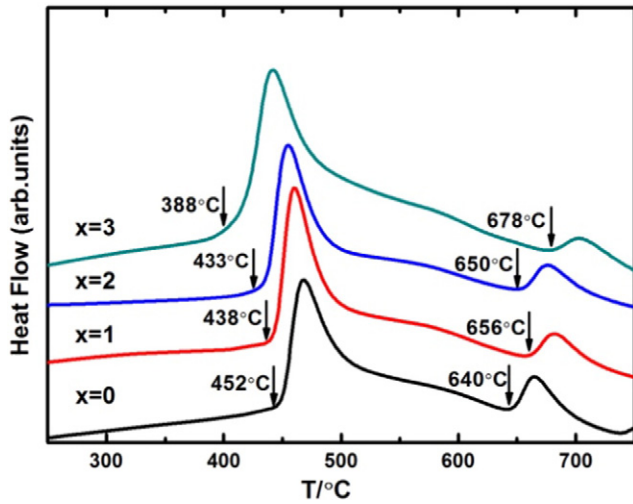


Fig. 1. DSC curves and crystallization temperatures of as-quenched $\text{Fe}_{65}\text{Co}_{15}\text{Si}_5\text{Nb}_3\text{Cu}_1\text{B}_{11-x}\text{Al}_x$ ($x = 0, 1, 2, 3$) alloys.

Table 1

Values of the onset primary and secondary crystallization temperatures (T_{x1} and T_{x2}), the interval temperature ΔT_x ($\Delta T_x = T_{x2} - T_{x1}$), as well as the Curie temperature (T_c^{am}) for as-quenched $\text{Fe}_{65}\text{Co}_{15}\text{Si}_5\text{Nb}_3\text{Cu}_1\text{B}_{11-x}\text{Al}_x$ ($x = 0, 1, 2, 3$) alloys.

Alloys	$T_{x1}/^\circ\text{C}$	$T_{x2}/^\circ\text{C}$	$\Delta T_x/^\circ\text{C}$	$T_c^{am}/^\circ\text{C}$
$x = 0$	451.9 ± 0.8	639.9 ± 0.6	188 ± 1.4	410 ± 2
$x = 1$	438.2 ± 0.8	655.9 ± 0.7	218 ± 1.5	390 ± 2
$x = 2$	433.3 ± 0.7	650.3 ± 0.7	217 ± 1.4	380 ± 1
$x = 3$	388.4 ± 0.6	678.0 ± 0.7	290 ± 1.3	360 ± 1

the differential scanning calorimetry (DSC) with a heating rate of $10^\circ\text{C}/\text{min}$ from room temperature to 1000°C .

3. Results and discussion

Differential scanning calorimetry (DSC) thermograms performed at $10^\circ\text{C}/\text{min}$ for the as-quenched $\text{Fe}_{65}\text{Co}_{15}\text{Si}_5\text{Nb}_3\text{Cu}_1\text{B}_{11-x}\text{Al}_x$ ($x = 0, 1, 2, 3$) alloys are shown in Fig. 1. For all samples, two separated exothermic peaks, which correspond to the two-stage crystallization process, were observed. The first one is correlated to the $\alpha\text{-FeCo(AlSi)}$ formation which is soft magnetic phase and the secondary one is associated with the subsequent precipitation of Fe–B hard magnetic phase. The onset primary temperature (T_{x1}), secondary crystallization temperature (T_{x2}) and the interval temperature (ΔT_x) for as-quenched $\text{Fe}_{65}\text{Co}_{15}\text{Si}_5\text{Nb}_3\text{Cu}_1\text{B}_{11-x}\text{Al}_x$ ($x = 0, 1, 2, 3$) alloys are shown in Table 1.

As is shown, the T_{x1} shows a reduced tendency with increasing Al content. Especially for the alloy with $x = 3$, it exhibits a lowest T_{x1} ($\sim 388^\circ\text{C}$), which is lower than other Fe-based or FeCo-based alloys ever reported [3,12] and indicating its potential applications in technology. Although T_{x2} and ΔT_x shows an unstable change with adding Al, they exhibit general enlarged tendency compared with the Al-free alloy. Particularly, the alloy with $x = 3$ owns the largest ΔT_x about 290°C , which provides the possibility of precipitating a single soft magnetic crystalline phase from amorphous matrix in a broad temperature range.

Fig. 2 (a) shows the μ_i - T curves of as-quenched $\text{Fe}_{65}\text{Co}_{15}\text{Si}_5\text{Nb}_3\text{Cu}_1\text{B}_{11-x}\text{Al}_x$ ($x = 0, 1, 2, 3$) alloys. A characteristic sharp Hopkinson peak was observed on all μ_i - T curves at the Curie point of the amorphous phase, T_c^{am} , from which we can get $T_c^{am} = 410, 390, 380$ and 360°C for the samples with $x = 0, 1, 2, 3$, respectively (see Table 1). The Curie temperature of amorphous phase (T_c^{am}) extracted from the μ_i - T curves of Fig. 2. (a) is shown in Fig. 2. (b). It can be observed that T_c^{am} decreased drastically from 440°C to 360°C with Al content increasing from $x = 0$ to $x = 3$. Panda et al. [13] clearly reported that the Curie temperature of Fe-based alloys was not strongly dependent on the metalloid, and we assumed this theory is also applied to FeCo-based alloys. Therefore, it can be deduced that the significant decrease in T_c^{am} is attributed to an increase of Al concentration in amorphous phase. Recently, Jia et al confirmed that Ni addition could decrease the T_c^{am} of FeCo-based Finemet-type alloy because of Ni consuming an amount of Fe in amorphous phase and ultimately diminishing the stronger exchange interaction between Fe and Co atoms largely [12]. The results of our experiment indicate that Al had a similar action with Ni on T_c^{am} of FeCo-based Finemet-type alloy, and we can also deduce that some metallic element could reduce T_c^{am} in FeCo-based Finemet-type alloys.

The initial permeability μ_i , as a structure-sensitive property, is an important parameter for the magnetic circuit design of electronic device. In order to analyze the effect of Al content on μ_i behavior of the alloys, μ_i - T curves of 550°C -annealed $\text{Fe}_{65}\text{Co}_{15}\text{Si}_5\text{Nb}_3\text{Cu}_1\text{B}_{11-x}\text{Al}_x$ ($x = 0, 1, 2, 3$) alloys are shown in Fig. 3. For all the samples, the Hopkinson peak vanishes when they are annealed at 550°C , indicating the formation of desired two-phase nanocrystal structure. The μ_i of samples with different Al content decreased at different rates around at T_c^{am} . For the alloys with $x = 0$ and $x = 2$, the similar characteristic is that μ_i decreased toward zero near at their T_c^{am} , although the falling rate of μ_i for alloy with $x = 2$ is relatively slower than that of Al-free alloy. It can be observed that the 550°C -annealed $\text{Fe}_{65}\text{Co}_{15}\text{Si}_5\text{Nb}_3\text{Cu}_1\text{B}_{10}\text{Al}_1$ alloy exhibited the maximum room-temperature μ_i (~ 2200), and the obvious difference compared with the above two alloys is that μ_i did not decrease to zero around T_c^{am} but maintained a certain value until about $T = 650^\circ\text{C}$, which indicates its improved high-temperature soft

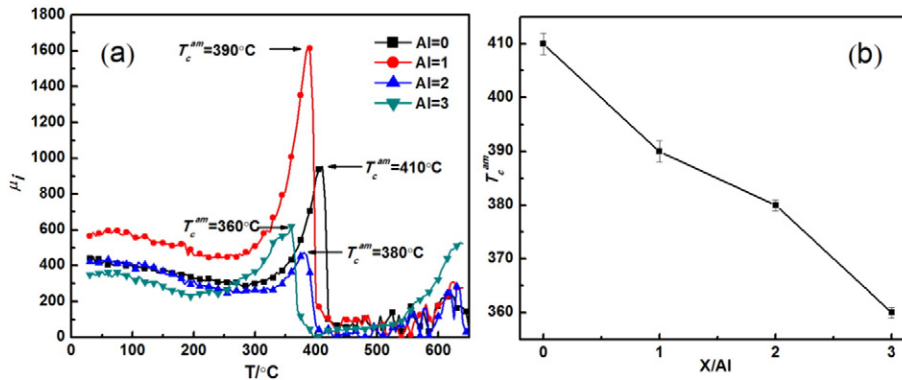


Fig. 2. (a) μ_i - T curves of as-quenched $\text{Fe}_{65}\text{Co}_{15}\text{Si}_5\text{Nb}_3\text{Cu}_1\text{B}_{11-x}\text{Al}_x$ ($x = 0, 1, 2, 3$) alloys. (b) The dependency of T_c^{am} , extracted from the μ_i - T curves of Panel (a), on Al content for $\text{Fe}_{65}\text{Co}_{15}\text{Si}_5\text{Nb}_3\text{Cu}_1\text{B}_{11-x}\text{Al}_x$ ($x = 0, 1, 2, 3$) alloys.

Download English Version:

<https://daneshyari.com/en/article/1480255>

Download Persian Version:

<https://daneshyari.com/article/1480255>

[Daneshyari.com](https://daneshyari.com)